Memoirs of the Faculty of Engineering, Nagoya University
Vol. 40, No. 1 (1988) -Research Report-

COMPETITIVE FORMATION OF NO AND N_2 FROM BOTH THE EMISSION SOURCES OF NH_3 AND COAL CHAR-BOUND NITROGEN COMPOUNDS DURING THE COMBUSTION OF COAL

NORIO ARAI and MASANOBU HASATANI

Department of Chemical Engineering

(Received May 13, 1988)

Abstract

The objective of this study is to basically elucidate a kinetic mechanism of formation of N_2 as well as NO through coal-bound nitrogen compounds during the combustion of coal. Two series of fundamental researches are conducted for this purpose. First the homogeneous gas-phase formation of NO and N_2 through NH_3 as a simulated model of volatile nitrogen compounds (volatile-N) evolved from coal is investigated in a mixture of NH_3, H_2, O_2, and Ar in a tubular flow reactor. Next a mathematical model is proposed for the competitive formation of NO and N_2 from both the emission sources of NH_3 and coal char-bound nitrogen (char-N) during the heterogeneous packed-bed combustion of coal-char particles under an NH_3/O_2/Ar gas stream.

The predictions of the proposed model are compared favorably with the experimental data for the transient formation and reduction of CO_2, CO, and NH_3, as well as of N_2 and NO. In addition, the relative contributions of volatile-NO (from volatile-N) and char-NO (from char-N) to total-NO emissions, and of volatile-N_2 and char-N_2 to total-N_2 emissions are revealed both theoretically and experimentally.

1. Introduction

One of the most vital problems to be cleared in the development of coal combustion units would be the abatement of total nitrogen oxide emissions. A considerable body of research work has been aimed at elucidating a kinetic mechanism of fuel-NO formed

through coal-bound nitrogen compounds during combustion. This is because fuel-NO was found to be the major contribution to total-NO emissions in practical combustors for coal.

Recent experimental works[4),11),12)] have shown that fuel-NO consists of volatile-NO and char-NO: the former originates from volatile nitrogen compounds (volatile-N) such as NH_3 and HCN, while the latter is from char-bound nitrogen in coal (char-N). In addition, following was generally accepted, namely, in the early stage of coal combustion, coal-bound nitrogen releases into the gas-phase in the form of NH_3, HCN, and the other gaseous nitrogen compounds with larger molecular weight. The remaining nitrogen in coal (char-N) reacts heterogeneously with surrounding gas products. All the nitrogen in coal is converted finally into N_2 and fuel-NO via. such two routes of reaction scheme in an air-rich combustion.

Although intensive efforts have been devoted to the identification of an intermediate nitrogen compound such as NH_3, and to experimental separation between volatile-NO and char-NO, scant attention has been paid to the kinetic mechanism of N_2 formation from coal-bound nitrogen. Exceptions have been found in recent works: Seidle and Branch[13)] measured the concentration profiles of chemical species involving N_2, NO, and OH in the NH_3-NO-O_2 reaction in postflame gases. With respect to coal combustion, Cliff and Young[7)] detected various kinds of gaseous nitrogen products like N_2, NO, NH_3, and HCN from the combustion of domestic coals under fuel-lean and fuel-rich conditions. They, however, have not suggested a comprehensive kinetic model so as to understand the characteristics of NO and N_2 formation in practical combustors for coal. In order to establish a low-NOx combustion techinque for coals, it is quite necessary to elucidate not only the kinetic mechanism of simultaneous formation of volatile-NO and char-NO but also that of formation of N_2 which may occur competitively with the NO-formation.

This work was focussed particularly on mathematical modeling for the competitive formation of NO and N_2 from both the emission sources of NH_3 and coal char-bound nitrogen during combustion. Following two series of fundamental researches were conducted for these purposes. First the homogeneous gas-phase formation of NO and N_2 through NH_3 as a simulated model of volatile nitrogen compounds evolved from coal was investigated in a mixture of NH_3, H_2, O_2, and Ar in a tubular flow-reactor. Next, based on these gas-phase reaction kinetics and a kinetic model[2)] for the formation of char-NO during the combustion of a single particle of coal char as well, a mathematical model was proposed for the competitive formation of NO and N_2 from NH_3 and char-N during the heterogeneous packed-bed combustion of coal-char particles under an $NH_3/O_2/Ar$ gas stream.

The validity of the proposed model is examined by comparing the experimental and the calculated results for the transient formation and reduction of CO_2, CO, and NH_3, as well as of N_2 and NO over the entire period of the packed-bed combustion of the char particles. In addition, the relative contributions of volatile-NO and char-NO to total-NO emissions, and of volatile-N_2 and char-N_2 to total-N_2 emissions are studied both theoretically and experimentally.

In this work, to avoid the formation of thermal-NO, a mixture of O_2 and Ar was employed as the oxidizer.

2. Theoretical Analysis

1. Mathematical modeling

1. 1. Combustion system to be analyzed and assumptions

Fig. 1 shows the geometric configuration of the present combustion system, in which

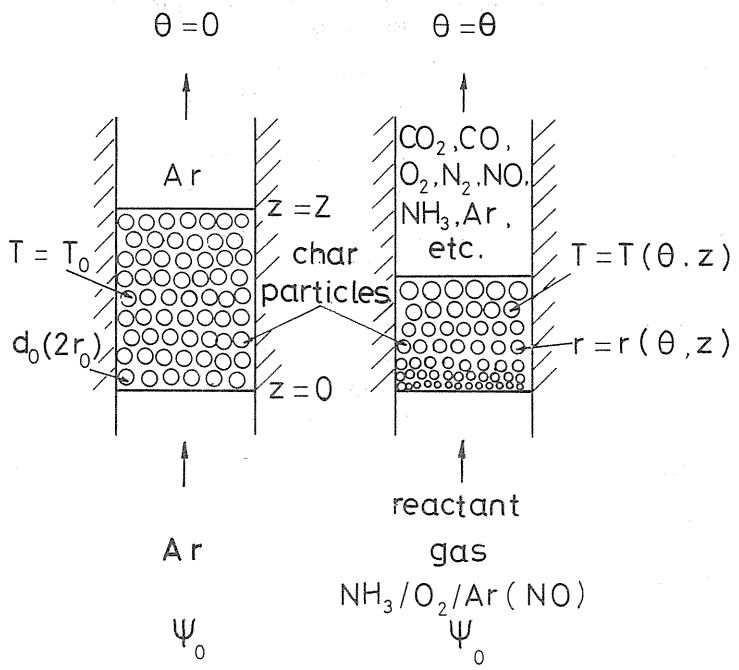

Fig. 1. Geometric configuration of the combustion system.

an $NH_3/O_2/Ar$ gas is introduced stepwise into a packed-bed of coal-char particles maintained at an initial temperature, T_0 under an inert Ar stream. After that time, heterogeneous char combustion and homogeneous gas-phase reactions have occurred continuously up to the completion of combustion. Following assumptions are made to simplify the present theoretical analysis.

1) Simultaneous formation of volatile-NO and char-NO in practical coal-combustion can be simulated by coupling two following reaction processes: (a) the char-NO formation from char-N in the char produced by the preliminary pyrolysis of parent coal, and (b) the volatile-NO formation through NH_3 as a simulated model of volatile-N evolved from the coal, 2) The overall reaction rate for the char-combustion is controlled by the surface reaction of char-C with oxygen, and no ash layer is left after the completion of combustion (an anthracite coal will be chosen as a parent coal), 3) Char-N is converted to NH as well as to NO at the surface of the particles, 4) Heterogeneous gas-solid reactions can be approximated by the proposed kinetic mechanism summarized in Table 1 and shown schematically in Fig. 2 as well, 5) The char particles are of spherical symmetry. The heat and mass transfer resistance of the particle is taken into account solely on the boundary surface between the particle and its surrounding reactant gas, 6) No thermal-NO is formed because an N_2-free gas is employed as the oxidizer, and 7) 18 chemical species are taken into consideration: CO_2, CO, N_2, O_2, H_2, NO, NO_2, H_2O, HO_2, HNO, NH_3, NH_2, NH, OH, H, O, N, and Ar, which are all ideal gases.

Table 1. Heterogeneous gas-solid reaction mechanism.

Reaction	Rate constant	Heat of reaction
1. $C+½O_2=CO$	$k_1=3.21\times10^{-3}\exp(-53.9/RT)$ $[g-C.cm^{-2}.s^{-1}.kPa^{-1}.]$	9.62 $[kJ.\ g^{-1}]$
2. $C+CO_2=2CO$	$k_2=5.9\times10^{-8}T^{-1}\exp(-247.7/RT)$ $[g-C.cm^{-2}.s^{-1}.kPa^{-1}.]$	−159.8
3. $C+H_2O=CO+H_2$	$k_3=1.33\times10^{3}T\ \exp(-147/RT)$ $[s^{-1}]$	−9.83
4. $C+NO=1/2N_2+CO$	$k_4=2\times10^{13}\exp(-227.6/RT)$ $[s^{-1}]$ for $T > 943$ K $k_4=2.33\times10^{4}\exp(-71.1/RT)$ for $T < 943$ K	
5. $H+¼O_2=½H_2O$		141.9
6. $N+½O_2=NO$		
7. NH (s)=NH (g)		

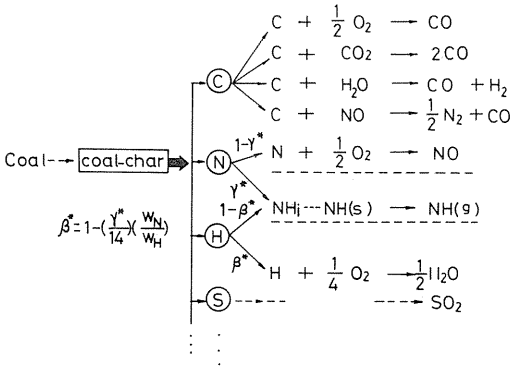

Fig. 2. Reaction mechanism of heterogeneous char combustion.

1. 2. Kinetic mechanism

Sixty mechanisms of heterogeneous and homogeneous reaction have been employed in the present theoretical analysis. These mechanisms are summarized in Tables 1 and 2 together with the rate constants.

Table 2. Homogeneous gas phase reaction mechanism and kinetic data. (k^+ : forward rate constant)

Reaction	$k^+=A\ T^n\ exp\ (-E/RT)$		
	A [cm^3, mol, s]	n	E [$kJ \cdot mol^{-1}$]
8. $CO+½O_2=CO_2$	Ref.9		
9. $CO+OH=CO_2+H$	Ref.3		
10. $CO+NO=½N_2+CO_2$	Ref.6		
11. $N+OH=NO+H$	4.10×10^{7}	0	0
12. $N+O_2=NO+O$	6.4×10^{3}	1.0	26.14
13. $N+NO=N_2+O$	1.55×10^{7}	0	0
14. $N+O+M=NO+M$	6.44×10^{10}	−0.5	0
15. $N+N+M=N_2+M$	2.97×10^{11}	−0.99	0
16. $H+O_2=OH+O$	2.24×10^{8}	0	70.27
17. $O+H_2=OH+H$	1.80×10^{4}	1.0	68.55
18. $H_2+OH=H_2O+H$	1.17×10^{3}	1.3	15.26
19. $OH+OH=H_2O+O$	6.3×10^{6}	0	4.56
20. $H_2+M=H+H+M$	2.23×10^{6}	0.5	387.4
21. $O+O+M=O_2+M$	1.9×10^{7}	0	−7.49
22. $OH+H+M=H_2O+M$	2.2×10^{16}	−2.0	0
23. $NH_3+M=NH_2+H+M$	1.78×10^{10}	0	385.0
24. $NH_3+H=NH_2+H_2$	1.26×10^{8}	0	92.12
25. $NH_3+OH=NH_2+H_2O$	4.0×10^{4}	0.68	4.57
26. $NH_3+O=NH_2+OH$	1.5×10^{6}	0	25.10
27. $NH_3+N=NH_2+NH$	2.1×10^{5}	0.5	96.83
28. $NH_3+O_2=NH_2+HO_2$	1.0×10^{6}	0	257.2
29. $NH_2+NH_2=NH_3+NH$	2.0×10^{5}	0.63	15.04
30. $NH_2+HNO=NH_3+NO$	5.0×10^{7}	0	4.18
31. $NH_2+OH=NH+H_2O$	3.0×10^{4}	0.68	5.49
32. $NH_2+H=NH+H_2$	1.0×10^{5}	0.67	17.95
33. $NH_2+O=NH+OH$	9.2×10^{5}	0.5	0
34. $NH_2+NO=N_2+H_2O$	9.12×10^{13}	−2.46	7.48
35. $NH_3+NO=HNO+NH$	1.0×10^{7}	0	167.2
36. $NH_2+O=HNO+H$	1.0×10^{5}	0	0
37. $NH+OH=N+H_2O$	1.6×10^{6}	0.56	−6.32
38. $NH+OH=NO+H_2$	1.6×10^{6}	0.56	6.28
39. $NH+O=N+OH$	1.0×10^{6}	0.5	0.42
40. $NH+O=NO+H$	5.0×10^{5}	0.5	20.95
41. $NH+O_2=NO+OH$	1.0×10^{4}	0	0
42. $NH+O_2=HNO+O$	1.0×10^{6}	0	13.59
43. $NH+NO=N_2+OH$	1.0×10^{7}	0	0
44. $NH+H=N+H_2$	1.0×10^{6}	0.68	7.98
45. $NH+NH=N_2+H_2$	4.0×10^{5}	0.55	7.98
46. $NH+N=N_2+H$	1.0×10^{7}	0	0
47. $H+HO_2=OH+OH$	2.5×10^{8}	0	7.98
48. $H+O_2+M=HO_2+M$	1.50×10^{9}	0	−4.14
49. $H+HO_2=H_2+O_2$	2.50×10^{7}	0	2.91
50. $H+HO_2=H_2O+O$	5.00×10^{7}	0	4.18
51. $HO_2+OH=H_2O+O_2$	1.0×10^{7}	0	0
52. $HO_2+O=OH+O_2$	4.80×10^{7}	0	4.18
53. $NO+HO_2=NO_2+OH$	1.0×10^{7}	0	0
54. $NO_2+H=OH+NO$	7.2×10^{8}	0	8.06
55. $NO_2+O=NO+O_2$	1.0×10^{7}	0	2.49
56. $HNO+OH=NO+H_2O$	3.6×10^{7}	0	0
57. $HNO+H=H_2+NO$	4.8×10^{6}	0	0
58. $HNO+H=NH+OH$	2.0×10^{5}	0.5	5.44
59. $HNO+M=H+NO+M$	3.0×10^{16}	0	203.5
60. $HNO+O=OH+NO$	1.0×10^{5}	0	0

(1) Heterogeneous gas-solid reactions: Seven mechanisms of the heterogeneous gas-solid reaction for the char combustion as shown in Tabel 1 are accounted for. Reactions 2 and 3 are the typical reactions of coal gasification, and reaction 4 is to be the main one for the NO-reduction by coal char.[5),6),8),10)] According to the same scheme as described in our prior paper,[2)] a mass fraction γ^* of the total char-N is released into the gas phase in the form of NH. The hydrogen in NH is compensated for by the fraction $(1-\beta^*)$ of the total char-H. The residual fraction of char-N, $(1-\gamma^*)$, and of char-H, β^*, are oxidized to NO and H_2O, respectively.

(2) Homogeneous gas-phase reactions: Reactions 8 through 60 in Table 2 are postulated to occur outside of the particle of char. In this work, however, homogeneous hydrocarbon combustion which may take place in practical combustors for coal is not accounted for. The rate expressions and the rate constants for reactions 8 to 10 have been taken from the literature.[3),6),9)] Reactions 11 to 60 have been extracted from the full kinetic model[1),13)] for the gas-phase reaction in an NH_3-H_2-NO-O_2-Ar mixture.

1. 3. Basic equations

Rate equation of heterogeneous gas-solid reaction: The overall oxidation rate of char-C in a spherical particle is expressed as

$$\bar{R}_C=-\frac{\rho_p W_c}{3}\frac{dr}{d\theta}=\frac{P_{O_2}}{(1/k_1)+(1/k_D)} \tag{1}$$

In the same manner as described in a previous paper,[2)] the overall rates of release of char-H, char-N, and char-NH into the gas phase are given as follows:

$$\bar{R}_H=(\beta^* W_H/W_C)\ \bar{R}_C \tag{2}$$

$$\bar{R}_N=[(1-\gamma^*)W_N/W_C]\ \bar{R}_C \tag{3}$$

and

$$\bar{R}_{NH}=(\gamma^* W_N/W_C)\ \bar{R}_C \tag{4}$$

Rate equation of homogeneous gas-phase reaction: A net formation rate of the target species Y_k is

$$r_k=\frac{dC_{Y_k}}{d\theta}=F_i\ (\theta,\ C_{Y_k}) \qquad (k=1,\ 2,\ \ldots\ldots\ m) \tag{5}$$

In the same way we can introduce the rate equations for m species (Y_1, Y_2, ... Y_m) to be analyzed.

Energy conservation equation: The time-history of the temperature of the particles during combustion can be expressed as

$$c_P\rho_P\ (1-\varepsilon_B)\ \frac{\partial T}{\partial\theta}=\lambda_e^o\frac{\partial^2 T}{\partial z^2}+h_P a_P(\psi-T)+a_P\sum_{j,\ n}(H_n\bar{R}_{S_j}) \qquad (6)$$
$$(S_j=\text{char-C, char-H, char-N, char-NH})$$

where n is the number of reaction mechanism listed in Tables 1 and 2.

The heat transfer equation controlling the temperature field of the reactant gas flowing the void space of the bed is given as follows:

$$c_g\rho_g\varepsilon_B\ \frac{\partial\psi}{\partial\theta}+c_g\rho_g u_g\ \frac{\partial\psi}{\partial z}=\lambda_g\frac{\partial^2\psi}{\partial z^2}-h_P a_P(\psi-T)+\varepsilon_B\sum_{k,\ n}(H_n r_{Y_k}). \quad (7)$$

Mass conservation equation: The mass conservation equation of each species (totally 18 species) is introduced on the basis of mass balance of the species. With respect to the species Y_k,

$$\varepsilon_B\ \frac{\partial C_{Y_k}}{\partial\theta}+u_g\ \frac{\partial C_{Y_k}}{\partial z}=D_{Y_k}\ \frac{\partial^2 C_{Y_k}}{\partial z^2}+\varepsilon_B r_{Y_k}+a_p\sigma\left(\frac{\bar{R}_{S_j}}{M_{S_j}}\right) \qquad (8)$$

where

$$\sigma=1 \text{ at } \quad (Y_k,\ S_j)=(\text{CO, char-C}),\ (\text{NO, char-N}),\ (\text{NH, char-NH}),\ (\text{H}_2\text{O, char-H}) \qquad (9)$$

and

$$\sigma=0 \text{ at } \quad Y_k\neq\text{CO, NO, NH, H}_2\text{O}$$

is obtained.

By solving the simultaneous differential equations thus introduced under the given initial and boundary conditions, we can predict the time-histories of the temperatures of the particles and gas, and the concentrations of all the species.

3. Experimental

Figs. 3 and 4 are two sorts of experimental apparatus employed in the present work. Only the main reaction part of the experimental apparatus for the char-combustion experiments is shown in detail in Fig. 3. A preheated NH_3/Ar gas was introduced into the inner tube of a concentric double reaction tube, while an O_2/Ar gas as the oxidizer flowed the annular space between the two tubes. A well-mixed reactant gas entered into a packed-bed of the char particles with sintered porous quartz-plate on its bottom.

Taisei coal (an anthracite from China) was devolatilized preliminarly in an evacuated atmosphere at a temperature of 1373 K to produce sample coal char: ultimate analysis of the char gives as C=93.65, H=0.1, N=0.34, S=0.35, O=0.1, and ash=5.46 % on a dry

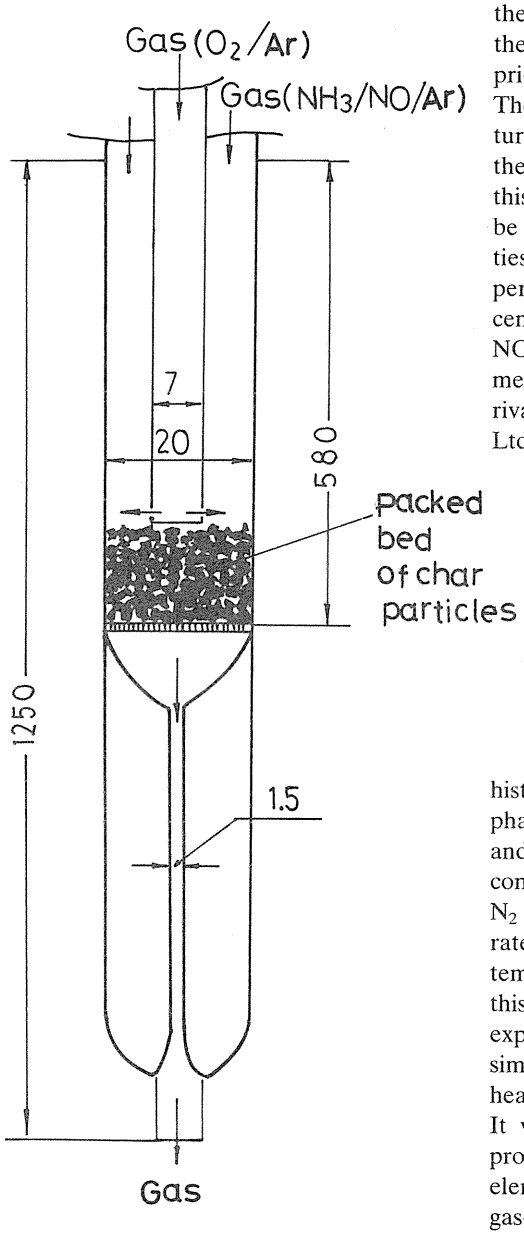

Fig. 3. Details of main reaction vessel of the experimental apparatus employed for char combustion experiment.

basis. On the other hand, Fig. 4 is a schematic drawing of the experimental apparatus for the gas-phase reaction experiments without the char particles, which were performed prior to the char-combustion experiments. The typical examples of measured temperature distributions along the axial direction of the reaction tube are shown in Fig. 5. From this figure, the temperature field appears to be of almost isothermal except in the vicinities of both ends of the tube. In every experimental run, the time-histories of the concentrations of CO_2, CO, N_2, NH_3, O_2, and NO at the exit of the reaction tube were measured continuously by a high-order derivative spectro-photometer (Yanagimoto Co. Ltd., UO-1 type) and gas-chromatograph.

4. Results and Discussion

1. Gas-phase reaction in a mixture of NH_3, H_2, O_2 and Ar gas

Fig. 6 represents the calculated time-histories of product species due to the gas-phase reaction in a mixture of NH_3, H_2, O_2 and Ar without the char particles. The final concentrations of the species such as NO and N_2 are influenced strongly by the heating-up rate of the reactant gas even if a terminal temperature is the same. In order to check this point experimentally, Fig. 7 compares experimental data (symbols) with model simulation (curve) in which the effect of the heating-up rate was taken into consideration. It was found from this comparison that the proposed reaction model based on elementary reaction kinetics can describe the gas-phase reaction in a mixture of NH_3, H_2, O_2 and Ar gas. In addition, it was revealed in the temperature range of 970 to 1400 K employed that, 1) the main product of the decay of NH_3 is N_2, while NO formation is relatively scant, and 2) the formation rate of N_2 from NH_3 is enhanced by the coexistence of H_2.

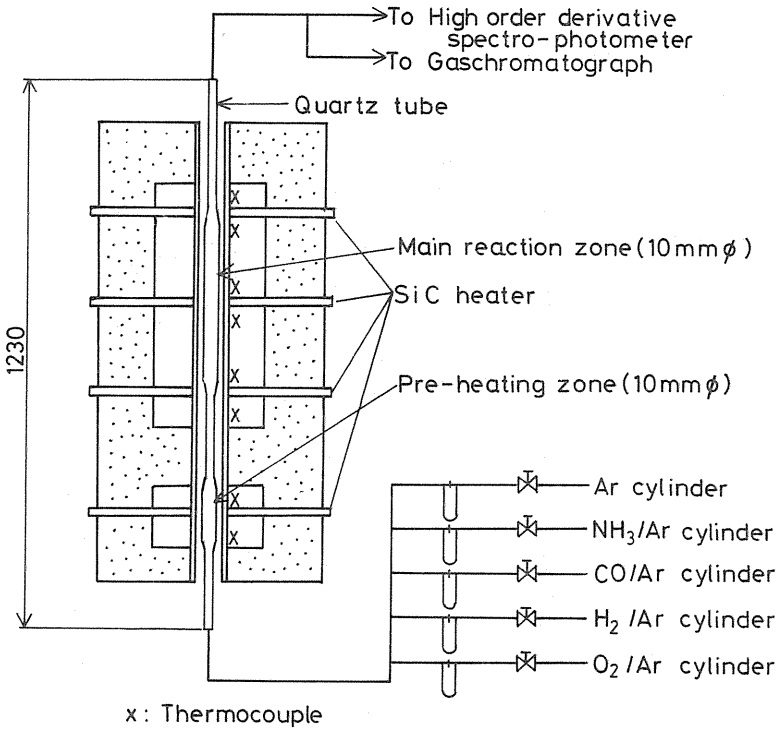

Fig. 4. Schematic drawing of experimental apparatus for gas-phase reaction experiment.

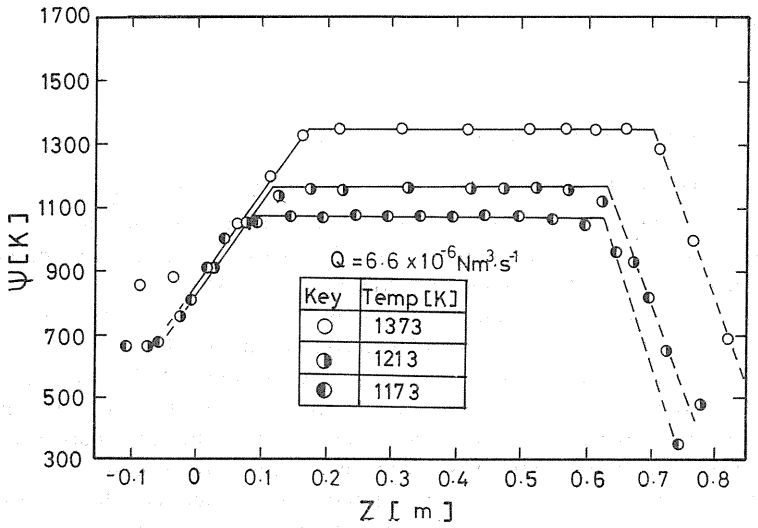

Fig. 5. Temperature distribution of reactant gas.

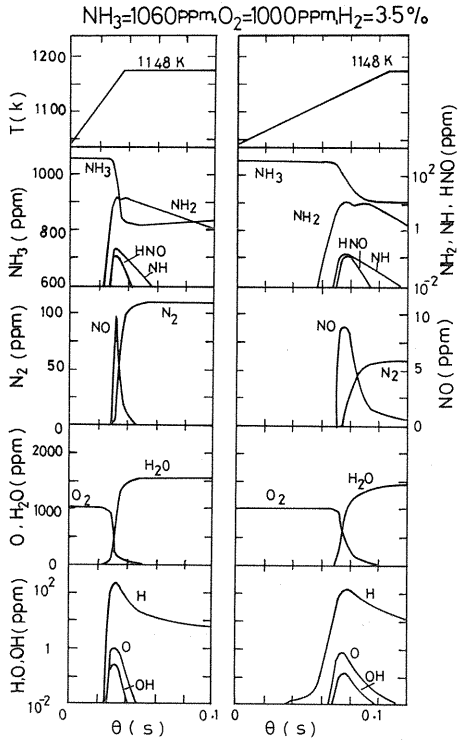

Fig. 6. Calculated time-histories of product species due to the gas-phase reaction in a mixture of NH_3, H_2, O_2 and Ar gas without the char particles.

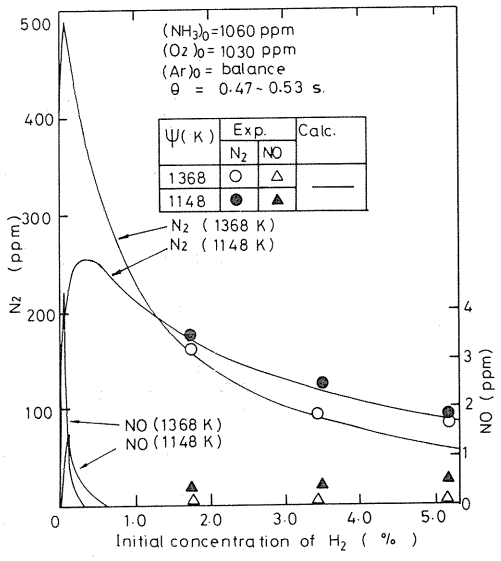

Fig. 7. Effects of initial concentration of H_2 and reaction temperature on the formation of NO and N_2.

2. *Packed-bed combustion of the char particles*

2. 1. *Comparison between calculated results and experimental data*

In order to validate the present theoretical analysis from more advanced standpoint of view, the calculated results were compared with the experimental data for the packed-bed combustion of the char particles under an $NH_3/O_2/Ar$ gas stream.

Fig. 8 shows a typical example of comparisons of the calculated results with the experimental data for the time-histories of the concentrations of CO_2, CO, O_2, N_2, and NO at the exit of the bed, but in the absence of initial-NH_3. In the theoretical calculation, the value of γ^* was determined experimentally by the same method as described in our prior paper,[2] of which the value is 0.01 for the char particles employed. As can be seen from Fig. 8, there exists a maximum for both concentrations of NO and N_2. Incidentally, the NO and N_2 thus formed can be termed the "char-NO" and "char-N_2", respectively since both are obviously originated from coal char-bound nitrogen (char-N). These experimental trends involving the formation characteristics of CO_2, CO, and O_2 as the main products can be well-explained by the theoretical analysis based on the present kinetic mechanism.

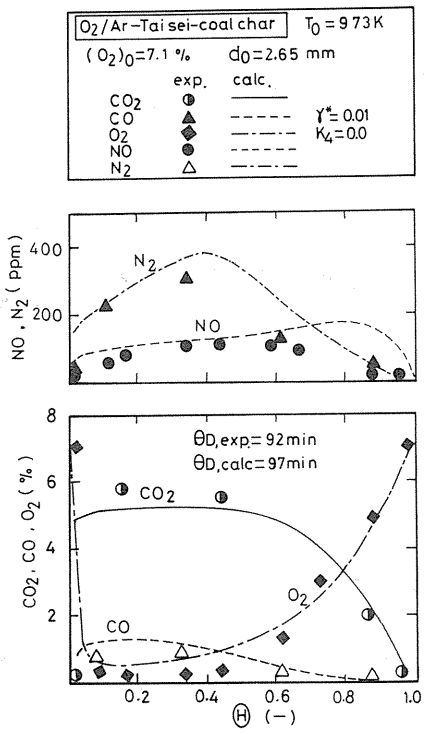

Fig. 8. Comparison between the present calculated results and the experimental data for time-histories of CO_2, CO, O_2, N_2 and NO during combustion in a char-O_2/Ar system.

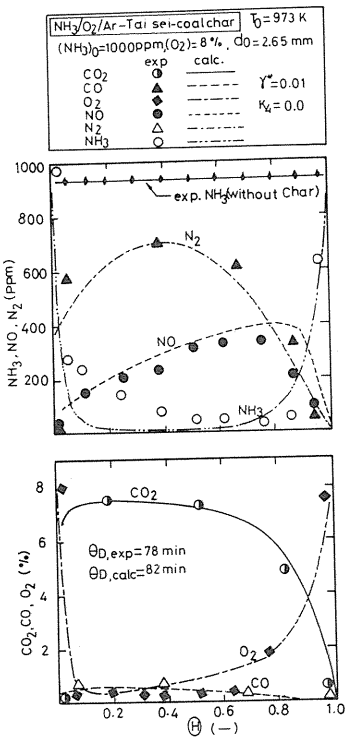

Fig. 9. Comparison between the present calculated results and the experimental data for simultaneous formation of volatile-NO and char-NO in a char-NH_3/O_2/Ar system.

The calculated time-histories of all the species measured in the presence of initial-NH_3 as a simulated model of volatile-N source were compared with the experimental data in Fig. 9, where the initial concentration of NH_3 was being kept at 1000 ppm over the entire period of combustion. The time-history of NH_3 measured in the absence of the char particles (empty bed) is also plotted in Fig. 9. It was revealed from the experimental results that, 1) the presence of the char particles enhances the decay rate of NH_3, 2) the time-dependent formation curves of all the products except NH_3 are roughly similar in shape with those of in Fig. 8 (initial-NH_3 free system), and 3) the concentration levels of NO (=char-NO+volatile-NO) and N_2 are uprisen by the presence of NH_3. These experimental trends were compared favorably with the present theoretical model as seen from Fig. 9. Fig. 10 shows the calculated axial distributions of the temperature of the bed and the concentrations of reactant gases at $\Theta=0.4$ ($\Theta=\theta/\theta_D$). From this figure it was evident theoretically that, 1) the conversion of NH_3 into NO and N_2 takes place concurrently with the oxidation of char-C, and 2) there exists a maximum for the temperature profile in the axial direction of the bed.

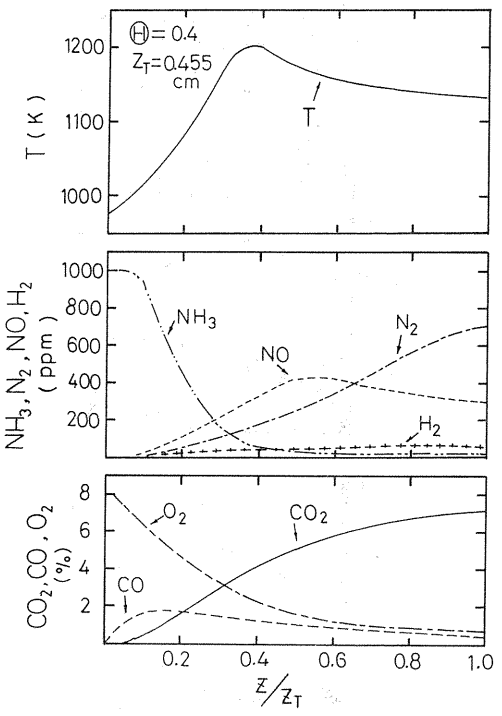

Fig. 10. Calculated axial-distributions of the temperature of the particles and the concentrations of product species at Θ=0.4: other conditions are the same as in Fig. 9.

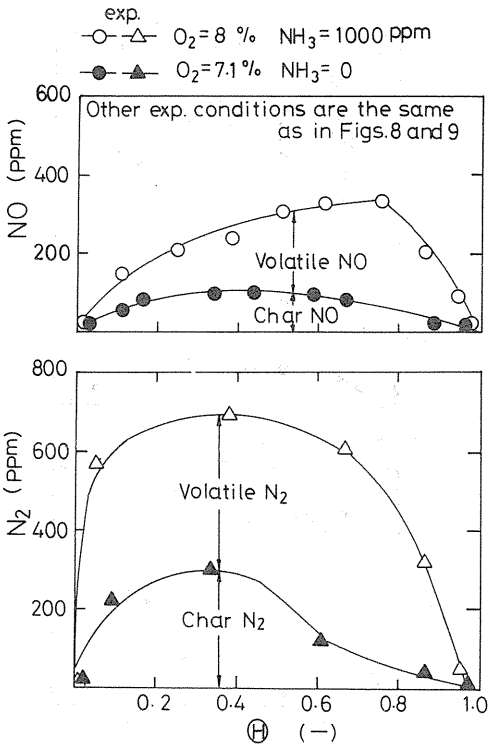

Fig. 11. Experimental separation between volatile-N_2 and char-N_2.

2. 2. *Separation between volatile-N_2 and char-N_2*

An experimental separation between volatile-N_2 and char-N_2 has not been succeeded so far. Fortunately, the present char-combustion experiments in the presence and absence of the initial-NH_3 facilitate to experimentally separate volatile-N_2 and char-N_2 from total-N_2 emissions. The time-histories of volatile-N_2 and char-N_2 extracted from the experimental data in Figs. 8 and 9 are plotted in Fig. 11, together with those of volatile-NO and char-NO. As far as the present reaction system may be concerned, volatile-N_2 is the major contribution to total-N_2 emissions. This experimental trend was confirmed theoretically by comparing with the calculated results as well (Figs. 8 and 9).

5. Conclusion

The following conclusions are drawn by the present study:

1) Within the temperature range between 970 and 1400 K in the absence of the char particles, the main product of the decay of NH_3 is N_2, while NO formation is relatively scant. However, the formation rate of N_2 from NH_3 is enhanced by the coexistence of H_2.
2) The presence of the char particles enhances strongly the decay rate of NH_3.
3) The formation rates of NO and N_2 from both the emission sources of volatile-N and char-N are controlled definitely by the oxidation rate of char-C.
4) The experimental separation between char-N_2 and volatile-N_2 may be succeeded.
5) These experimental trends of 1) to 4) can be explained well by the present theoretical analysis based on the proposed kinetic model.

Acknowledgement

The authors express many thanks to Dr. Y. Ninomiya (Tokyo Univ. of Agricul. & Tech.) and Mr. Y. Nakai (Toho Gas Co. Ltd.) for their assistance to this work. A part of this work was supported by the Grant-in-Aid for Science Research from the Ministry of Education, Science and Culture of Japan.

Nomenclature

A	frequency factor
a_p	specific surface area of the particles on bed volume basis (cm^{-1})
C	concentration of chemical species (mol. cm^{-3})
c	specific heat (kJ. g^{-1}. K^{-1})
D	diffusivity (cm^2. s^{-1})
d_0	initial diameter of the particle (cm)
E	energy of activation (kJ. mol^{-1})
H	heat of reaction (kJ. g^{-1}, kJ. mol^{-1})
h_p	heat transfer coefficient (W. cm^{-2}. K^{-1})
k_D	diffusional reaction rate constant (g−C. cm^{-2}. s^{-1}. kPa^{-1})
k_i	rate constant of i-th reaction
M	molecular weight (g. mol^{-1})
p	partial pressure (kPa)
Q	volumetric flow rate of reactant gas (N cm^3. s^{-1})
R	universal gas constant (cm^3. kPa. mol^{-1}. K^{-1}, kJ. mol^{-1}. K^{-1})
$\bar{R}$	reaction rate on area basis (g. cm^{-2}. s^{-1})
r	radius of the particle (cm)
r	net formation rate of gas (mol. cm^{-3}. s^{-1})
T	temperature of the particle (K)
u	linear velocity of gas (cm. s^{-1})
W	mass fraction of reactant component in char
Z	height of the bed (cm)
z	distance from the entrance of the bed (cm)

Greek symbols

β^*	characteristic parameter
γ^*	characteristic parameter
ε_B	void fraction of the bed
Θ	dimensionless reaction time ($=\theta/\theta_D$)
θ	reaction time (min.,s)
λ	thermal conductivity ($W.cm^{-1}.\ K^{-1}$)
ψ	temperature of gas (K)

Subscript

0	initial

References

1) Arai, N., Ninomiya, Y., Nakai, Y. and Hasatani, M.: Kagaku Kogaku Ronbunshu (Japanese), *12*, 393 (1986) and Intern. Chem. Eng., *28*, 344 (1988).
2) Arai, N., Hasatani, M., Ninomiya, Y., Churchill, S.W. and Lior, N.: 21st Symp. (Intl.) on Combustion, The Combustion Institute, p. 1207, 1986.
3) Baulch, D.L., Drysdale, D.D., Duxbury, M.A. and Grant, S.J.: Evaluated Kinetic Data for High Temperature Reactions, Vol. 3 (1976) Butterworth.
4) Béer, J.M. and Martin, G.B.: AIChE Symp. Ser., No.175, *74*, 93 (1978).
5) Béer, J.M., Sarofim, A.F. and Lee, Y.Y.: 6th Intern. Conf. on FBC, Vol.III, p. 942, 1980.
6) Chan, L.K., Sarofim, A.F. and Béer, J.M.: Combust. Flame, *52*, 37 (1983).
7) Cliff, D.I. and Young, B.C.: Fuel, *64*, 1521 (1985).
8) Furusawa, T., Tsunoda, M., Tsujimura, M. and Adschiri, T.: ibid., *64*, 1306 (1985).
9) Howard, J.B., Williams, G.C. and Fine, D.H.: 14th Symp. (Intl.) on Combustion, The Combustion Institute, p. 975, 1973.
10) Kunii, D., Wu, K.T. and Furusawa, T.: Chem. Eng. Sci., *35*, 170 (1980).
11) Pershing, D.W. and Wendt, J.O.L.: Ind. Eng. Chem. Process Des. Dev., *18*, 60 (1979).
12) Pohl, J.H. and Sarofim, A.F.: 16th Symp. (Intl.) on Combustion, The Combustion Institute, p. 491, 1977.
13) Seidle, J.P. and Branch, M.C.: Combust. Flame, *52*, 47 (1983).